IEIE Transactions on Smart Processing and Computing, vol. 3, no. 1, February 2014
http://dx.doi.org/10.5573/IEIESPC.2014.3.1.19

Multi-Resolution Kronecker Compressive Sensing

Thuong Nguyen Canh[1], Khanh Dinh Quoc[2], and Byeungwoo Jeon[3]

Department of Electronic and Electrical Engineering, Sungkyunkwan University / Suwon, South Korea
{ngcthuong, kqdinh, bjeon}@skku.edu

***** Corresponding Author: Byeunwoo Jeon

Received October 20, 2013; Revised October 31, 2013; Accepted November 15, 2013; Published February 28, 2014

** Regular Paper*

***Abstract*:** Compressive sensing is an emerging sampling technique which enables sampling a signal at a much lower rate than the Nyquist rate. In this paper, we propose a novel framework based on Kronecker compressive sensing that provides multi-resolution image reconstruction capability. By exploiting the relationship of the sensing matrices between low and high resolution images, the proposed method can reconstruct both high and low resolution images from a single measurement vector. Furthermore, post-processing using BM3D improves its recovery performance. The experimental results showed that the proposed scheme provides significant gains over the conventional framework with respect to the objective and subjective qualities.

***Keywords*:** Compressive imaging, multi-resolution, Total variation, Reconstruction, Split Bregman

1. Introduction

Recently, compressive sensing (CS) [1] has attracted considerable attention for its capability of simultaneous sampling and compression. CS allows, from a much smaller number of measurements, to reconstruct a signal by relying on the sparsity property of signals in some sparse domains (*i.e.*, DCT, DWT, gradient domain...). On the other hand, in case of multidimensional signals (*e.g.*, image or video), a frame-based CS has practical difficulties, such as high computational complexity or large memory requirements arising from the large number of measurements. In this regard, a block-based approach [2, 3] was developed but it missed the global characteristics of the images despite preserving the local ones. Duarte et al. introduced a Kronecker compressive sensing (KCS) scheme [4] that senses data in the frame-based manner but can reduce the complexity considerably using a Kronecker product.

A key challenge of CS towards practical applications is reducing the computational complexity of reconstruction. In general, the higher image resolution becomes, the larger computational complexity CS requires. A partial solution for this is a multi-resolution sensing framework that senses multi-resolution measurements and reconstructs a low resolution (LR) image, but later a high resolution (HR) image is reconstructed using a powerful reconstruction supported by sufficient computational complexity. This scheme has an added feature of providing a fast preview for real-time compressive image/video with a low-cost reconstruction of a low resolution (LR) image [11-13]. This can also provide benefits to many image processing tasks, such as image classification, object detection, *etc.* with little sacrifice in accuracy. For example, the initial object detection can be obtained from a low cost reconstructed LR image/video, and then enhanced from a reconstructed HR image/video.

CS is unable to provide a high quality reconstruction if its subrate is too low. Because CS takes a much smaller number of measurements via random projection, it is easy to miss important signal features. The loss of some high frequency signal components brings in consequential suffering of heavy staircase artifacts. Therefore, CS recovery has difficulty in reconstructing accurate HR images at a very low subrate. Conventional image/video compression faces similar problems in achieving a very high compression ratio while dealing with a HR image. One possible remedy is employment of down-sampling of the image/video sequences before compression and using a super resolution (SR) technique to up-sample the decompressed signal at the decoder [8]. SR is an image processing technique that can generate a HR image from a single or a set of LR images [8]. This scheme can be used for quality-bitrate control of a reconstructed HR in spatially scalable image/video coding.

One of the widely used CS reconstruction methods is

(a) TV[6]: 25.26dB (b) SRTV: 27.06dB (c) SRTV+BM3D^2: 28.96dB

Fig. 1. Recovered Lena image (512x512) from compressive sensing with a subrate of 0.05 (see Table 1).

the total variation (TV) technique [5-7], which can achieve good CS recovery performance while preserving edges of images well. However, in case of a very low subrate, such as 0.05, it has very poor recovery performance, as depicted in Fig. 1(a). Therefore, for a given low subrate, instead of sensing the original resolution (called high resolution (HR)) image, it might be better if the same sensing is performed to its spatially down-sampled (called low resolution (LR)) image, and the HR image is generated by up-sampling the CS reconstructed LR image. The super resolution (SR) technique can be used for up-sampling.

Motivated by this, the aim of this study is to sense a LR image and to utilize SR to achieve better HR without increasing the number of measurements. Fig. 1 illustrates such a possibility. Fig. 1(a) shows a CS reconstructed original resolution image of 512x512 (*i.e.*, HR image) at a low subrate of 0.05. Equivalent subrate of 0.2 (=0.05x4) is used to produce a LR image (256x256), and its reconstructed HR images are shown in Figs. 1(b) and (c) which are generated by up-sampling LR via a bi-cubic interpolation [16] (for the algorithm names in Fig. 1, see Table 1, which will be explained later). As shown in Figs. 1(b) and (c) in comparison with Fig. 1(a), the SR-assisted reconstructed HR image produces higher reconstruction quality.

This paper proposes a multi-resolution compressed sensing framework that allows images to be reconstructed at various resolutions. By exploiting the relationship between the measurements of LR and HR images, we propose a HR sensing matrix, which shares the same measurement vector with the sensing LR image. In addition, the proposed sensing scheme corresponds to the sensing spatially down-sampled image (*i.e.*, LR image) at a high subrate. That is, it senses the LR image using the same number of measurements originally associated with the HR image. A HR image is finally reconstructed from the LR image. The reconstructed images are refined further to remove staircase artifacts using a BM3D [9] filter through post-processing as reported in [10]. The proposed multi-resolution Kronecker compressive sensing scheme is simulated to verify its efficiency over the conventional KCS in both PSNR and perceptual quality.

The rest of this paper is organized as follows. Section II presents the background of the compressed sensing. The proposed multi-resolution sensing framework is delivered in section III. Numerical experiments are presented in section IV, and the paper is concluded in section V.

2. Background

This section first introduces the background of compressive sensing and then presents some related work.

2.1 Compressive Sensing

An emerging signal processing technique, CS allows acquiring signals with a much smaller sampling rate than the Shannon/Nyquist rate via a random projection. CS theory states that for a natural image, $f \in \mathbb{R}^{n^2 \times 1}$, which is sparse in a selected domain specified by a sparsifying matrix, Ψ, $f = \Psi\alpha$, it is possible to reduce its sampling cost by taking a much smaller number of measurements, $y \in \mathbb{R}^{m^2 \times 1}$, where $y = \Phi f$, and later reconstructing the signal f by solving the following optimization problem:

$$\hat{\alpha} = \operatorname{argmin}_{\alpha} \|\alpha\|_p \quad s.t. \; y = \Phi\Psi\alpha, \tag{1}$$

where $m^2 \ll n^2$, the notation $\|\cdot\|_p$ denotes the norm-p with p being normally set to either 0 or 1, and $\Phi \in \mathbb{R}^{m^2 \times n^2}$ is a sensing matrix which satisfies the restricted isometry property [1].

To reduce complexity caused by a large size of sensing matrix in multi-dimensional signals, Duarte and Baraniuk [4] presented Kronecker compressive sensing, which jointly models the sensing matrix for each signal dimension. For the 2D signal, $F \in \mathbb{R}^{n \times n}$, the sensing matrix is given as $\Phi = R \otimes G$, where $\otimes$ denotes the Kronecker product, R and $G^T \in \mathbb{R}^{m \times n}$ represent the sensing matrices for each dimension. Therefore, the CS measurement is rewritten as $Y = RFG$, where $y = vect(Y)$

is a vectorized version of the measurement matrix Y. The measurement constraint is:

$$\|\Phi f - y\|_2^2 = \|RFG - Y\|_2^2.$$

Under the framework of KCS, the optimization problem formulated as a total variation (TV)-based CS recovery [5-7] can be solved for the reconstructed signal:

$$min_F \; TV(F) + \frac{\mu}{2}\|RFG - Y\|_2^2, \tag{2}$$

where μ, γ are constant parameters and the total variation (an)isotropic for 2D discrete image are given as:

$$TV_{aniso}(F) = \|\nabla_x F\|_1 + \|\nabla_y F\|_1,$$
$$TV_{iso}(F) = \sum_{i,j}\sqrt{\left|(\nabla_x F)_{i,j}\right|^2 + \left|(\nabla_y F)_{i,j}\right|^2},$$

where ∇_x and ∇_y denote the gradient operators in the horizontal and vertical direction. Using the split Bregman technique [5], Eq. (2) can be solved more easily by replacing $V = F$, $D_x = \nabla_x F$, $D_y = \nabla_y$, and adding parameters B_x, B_y, and W as follows:

$$\min_{F,V,D_x,D_y} TV(F) + \frac{\mu}{2}\|RFG - Y\|_2^2 + \frac{\nu}{2}\|F - V - W\|_2^2 + \frac{\lambda}{2}\|D_x - \nabla_x V - B_x\|_2^2 + \frac{\lambda}{2}\|D_y - \nabla_y V - B_y\|_2^2, \tag{3}$$

where λ and ν are constant parameters. Eq. (3) can be split further into sub-problems F, V, D_x, D_y, which can be solved via eigen-decomposition and shrinkage function [6].

2.2 Related Work

The problem of multi-resolution CS has attracted high-level of attention recently. Park *et al.* presented a multi-scale framework for compressive video sensing [17], which can obtain LR and HR reconstructed images at the recovery side. On the other hand, this framework requires that compressive measurements are sampled at multiple scales for each video frame. Towards practical video compressive sensing, Baraniuk *et al.* proposed a dual scale sensing matrix (DSS) in CS-MUVI framework [12], which can generate an efficiently computable low-resolution video pre-view. To reduce computational complexity further, Goldstein *et al.* [13] proposed a new multi-resolution framework based on the STOne transform. In addition, the DSS was exploited further to provide spatially scalable compressive sensing [11]. These algorithms were designed for a single pixel camera imaging system [14], in which the elements of the sensing matrices are chosen either +1 or -1 to achieve easier and fast implementation. In the present approach, the HR sensing matrix is created based on the LR sensing matrix, which can be generated arbitrarily, like any other sensing matrices, such as random Gaussian sensing matrix, *etc*.

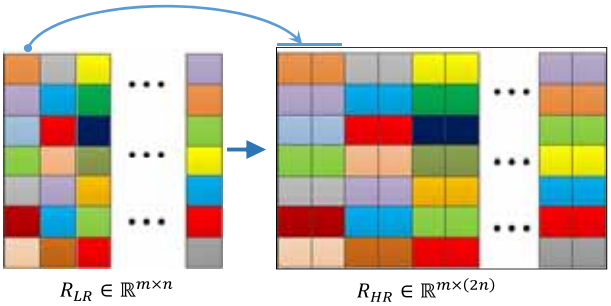

Fig. 2. Relationship between the HR and LR sensing matrices.

While related works [11-13, 17] were proposed for a normal CS framework, the proposed sensing scheme was significantly different in that it was under the KCS framework [4]. Moreover, while the approach [11, 12] sacrifices the performance of the recovered LR to have multi-resolution capability, in contrast to this approach, the proposed method reconstructs LR at a high reconstruction quality and then uses the SR technique to improve the HR quality. An approach of using SR to improve performance for exploiting predictive coding in spatially scalable compressive imaging has been reported [11], but it senses the HR and LR measurements separately and reconstructs them independently. In contrast, the proposed algorithm in this paper shares the same measurements between HR and LR, and reconstructs the HR and LR images jointly.

3. Proposed Multi-Resolution Kronecker Compressive Sensing

In this section, we first present a relationship between sensing matrices of high and low resolution images, and outline the proposed multi-resolution sensing matrices. The proposed reconstruction will be given in the later part.

3.1 Multi-resolution CS Acquisition

As mentioned in [13], the multi-resolution CS is desirable for enabling a fast preview of an image/video. Unfortunately, the conventional KCS framework [4] does not support the multi-resolution measurements. In general, KCS measurements of the same image at different resolutions (HR and LR) can be obtained by the following:

$$Y_{LR} = R_{LR}F_{LR}G_{LR}, \tag{4}$$
$$Y_{HR} = R_{HR}F_{HR}G_{HR}, \tag{5}$$

where Y_{HR} and Y_{LR} denote the measurement matrices of the HR ($F_{HR} \in \mathbb{R}^{2n\times 2n}$) and LR image ($F_{LR} \in \mathbb{R}^{n\times n}$) obtained by the corresponding sensing matrices, R_{LR}, $G_{LR}^T \in \mathbb{R}^{m\times n}$ and R_{HR}, $G_{HR}^T \in \mathbb{R}^{m\times(2n)}$, respectively.

To support the proposed multi-resolution measurement (that is, the same measurements shared by HR and LR), it is important to carefully design the sensing matrices so that the images can be reconstructed at different resolutions from the same set of measurements. In addition, it is better to design sensing matrices to be fully compatible with the conventional KCS without any modification of the sensing and recovering parts. Therefore, the relationship between the HR and LR sensing matrices should be investigated carefully. For that purpose, the LR and HR images are obtained via down-sampling operation as follows:

$$F_{LR} = D_S F_{HR} D_S^T,$$
$$D_S = \frac{1}{2}\begin{bmatrix} 1 & 1 & 0 & 0 & \cdots & 0 & 0 \\ 0 & 0 & 1 & 1 & & 0 & 0 \\ \vdots & & & & \ddots & \vdots & \\ 0 & 0 & 0 & 0 & \cdots & 1 & 1 \end{bmatrix} \in \mathbb{R}^{n \times 2n} \quad (6)$$

where D_S is a down-sampling matrix, F_{LR} is a bi-linear down-sampled version of F_{HR}, and the $(.)^T$ operator stands for a transpose operator. By setting $Y_{LR} = Y_{HR}$, the HR sensing matrix can be derived from the LR sensing one as follows:

$$\begin{aligned} R_{HR} F_{HR} G_{HR} &= R_{LR} F_{LR} G_{LR} = R_{LR}(D_S F_{HR} D_S^T) G_{LR}, \\ &= (R_{LR} D_S) F_{HR} (D_S^T G_{LR}), \\ \Rightarrow R_{HR} &= R_{LR} D_S;\ G_{HR} = D_S^T G_{LR}, \end{aligned} \quad (7)$$

Fig. 2 shows the relationship between the two sensing matrices. Using this HR sensing matrix (called LSM), the LR image and HR image can be reconstructed with the same set of measurements. Note that the use of the HR sensing matrix in (7) is equivalent to the sensing LR image at a high subrate. Therefore, we discard the high frequency component (*i.e.*, textures) at the sensing part. By keeping the same number of measurements, if a subrate of the sensing HR image is r, then the subrate for the LR image is $r \times 2^2$. As a result, the proposed sensing matrix prefers a subrate smaller than 0.25 because the subrate of LR becomes 1. Otherwise, the additional measurements will be wasted.

3.2 Multi-Resolution CS Reconstruction

Because HR and LR image sensing is designed to share the same measurements, reconstructing the HR and LR images is straightforward using TV[6] without modification. This is the conventional sensing and recovery method (called TV in Table 1). On the other hand, in this paper, the LR image is reconstructed first from the measurements, Y_{LR}, using the sensing matrices R_{LR}, G_{LR}, and the SR technique, such as bi-cubic interpolation [16], is applied simply to the LR image to generate the HR image; this is denoted by the Super-Resolution-assisted Total Variation reconstruction (SRTV) in Table 1. Thanks to the SR technique, we are able to obtain some details in the reconstructed HR image. The better SR algorithm is expected to show higher performance.

Table 1. Description of the reconstruction algorithms.

Algorithm	Descriptions
TV[6]	Conventional TV recovery [6] based on KCS.
SRTV*	SR-assisted TV reconstruction: recover LR by TV [6], then use SR to obtain HR.
SRTV+BM3D*	Post-process recovered LR by BM3D before using SR to obtain HR.
SRTV+BM3D^2*	Dual BM3D post-processing for SRTV: after recovery by SRTV+BM3D, apply post filter BM3D again to HR

Proposed (*)

Table 2. Description of the post processing algorithm [10].

Input: Initial image F^0, Y, sensing matrices R, G.
Output: F_S^{i+1} image.
Estimate image: $F_S^0 = \text{BM3D}(F^0)$, $i = 0$.
While $(i < 10)\&\big((ssim(i+1) - ssim(i)) < tol\big)$
$Y_{res} = Y - RF_S^i G$,
$F_{res}^i = TVrec(Y_{res}, R, G)$,
$\tilde{F}_S^{i+1} = F_S^i + F_{res}^i$,
$F_S^{i+1} = \text{BM3D}(\tilde{F}_S^{i+1})$,
$ssim(i+1) = \text{SSIM}(F_S^{i+1}, F_S^i)$,
$i = i + 1$,
End

Both LR and HR images contain significant staircase artifacts. This drawback was overcome by post-processing [10], which implements the BM3D [9]. By reconstructing the residual image by iterative filtering, the staircase artifact can be removed effectively due to the structure-preserving properties of the BM3D filter. The details of the algorithm are presented in Table 2. The structural similarity SSIM [15] between the two consecutive iterations is selected as the stopping because the aim was to preserve the nonlocal structure. The BM3D post-processing scheme was used after reconstructing the LR image, and then apply the SR technique was then applied; the algorithm is called SRTV+BM3D. Moreover, because the HR sensing matrices (R_{HR}, G_{HR}) can be obtained using (7), the reconstructed HR image of (SRTV+BM3D) can be refined further by BM3D post processing. This scheme is called SRTV+BM3D^2 in Table 1. By iteratively removing the staircase artifact in both the low and high resolution images, the proposed SRTV+BM3D^2 is expected to achieve the highest reconstruction performance.

4. Experimental Results

In this section, the effectiveness of the proposed idea of

Table 3. Performance comparison of various algorithms in PSNR and SSIM.

Image	Sub rate	BCS-SPL[2]		TVAL3[18]		TV[6]		SRTV*		SRTV+BM3D*		SRTV+BM3D^2*	
		PSNR	SSIM	PSNR	SSIM	PSNR	SSIM	PSNR	SSIM	PSNR	SSIM	PSNR	SSIM
Lena	0.05	25.38	0.739	22.78	0.616	25.23	0.705	27.06	0.756	28.10	0.786	28.87	0.777
	0.10	28.03	0.804	25.80	0.706	28.06	0.770	30.14	0.829	30.88	0.846	32.21	0.838
	0.15	29.89	0.842	28.08	0.773	29.71	0.810	32.14	0.874	32.42	0.876	34.06	0.873
	0.20	31.35	0.864	29.73	0.820	31.06	0.839	33.55	0.903	33.31	0.892	35.15	0.897
	0.25	32.46	0.887	31.21	0.854	32.19	0.860	34.45	0.924	33.78	0.901	35.77	0.914
Barbara	0.05	21.58	0.580	20.46	0.487	20.85	0.498	22.42	0.582	22.99	0.619	22.94	0.740
	0.10	22.57	0.640	21.98	0.562	22.30	0.555	23.84	0.665	24.43	0.707	24.64	0.839
	0.15	23.37	0.685	22.86	0.818	23.18	0.597	24.64	0.725	25.01	0.756	25.39	0.899
	0.20	24.16	0.722	23.53	0.666	23.97	0.638	25.20	0.775	25.25	0.779	25.62	0.929
	0.25	24.90	0.755	24.12	0.706	24.90	0.673	25.36	0.809	25.36	0.790	25.69	0.944
Peppers	0.05	25.66	0.736	22.01	0.585	25.25	0.707	26.79	0.761	27.79	0.787	28.64	0.815
	0.10	28.96	0.796	25.40	0.675	28.59	0.771	29.50	0.825	30.06	0.833	31.10	0.868
	0.15	30.78	0.827	27.86	0.742	30.41	0.804	30.69	0.856	30.88	0.852	31.97	0.891
	0.20	32.02	0.848	29.83	0.791	31.85	0.805	31.43	0.875	31.30	0.863	32.42	0.906
	0.25	32.95	0.864	31.57	0.829	32.91	0.849	31.86	0.894	31.52	0.869	32.68	0.917
Camera-man	0.05	23.03	0.750	21.88	0.634	24.93	0.747	26.59	0.794	27.88	0.826	28.83	0.910
	0.10	25.97	0.826	25.16	0.754	28.11	0.822	30.38	0.880	31.41	0.896	33.03	0.953
	0.15	28.41	0.873	27.51	0.823	30.33	0.865	32.97	0.928	33.34	0.928	35.36	0.969
	0.20	30.43	0.904	29.52	0.873	32.08	0.895	34.83	0.956	34.61	0.947	37.01	0.980
	0.25	32.12	0.925	31.08	0.903	33.48	0.913	36.40	0.975	35.39	0.957	38.15	0.988
Goldhill	0.05	24.27	0.598	23.18	0.535	23.99	0.559	25.38	0.612	25.77	0.623	26.06	0.662
	0.10	26.91	0.676	25.67	0.630	26.12	0.642	27.78	0.712	28.02	0.724	28.62	0.760
	0.15	28.04	0.726	27.16	0.693	27.34	0.694	29.46	0.780	29.47	0.770	30.29	0.816
	0.20	28.90	0.761	28.39	0.744	28.38	0.738	30.75	0.831	30.48	0.822	31.45	0.854
	0.25	29.67	0.792	29.37	0.782	29.29	0.772	31.64	0.865	31.11	0.840	32.19	0.881
Boats	0.05	22.97	0.586	21.46	0.515	22.53	0.547	23.98	0.604	24.39	0.621	24.74	0.642
	0.10	25.25	0.665	24.02	0.613	24.75	0.628	26.49	0.708	26.94	0.724	27.72	0.720
	0.15	26.65	0.717	25.63	0.680	26.16	0.684	28.26	0.781	28.52	0.786	29.59	0.776
	0.20	27.77	0.756	26.98	0.731	27.40	0.729	29.48	0.832	29.43	0.822	30.59	0.811
	0.25	28.68	0.787	28.22	0.773	28.46	0.766	30.21	0.862	29.87	0.840	31.04	0.829
Average		27.44	0.764	26.08	0.710	27.46	0.729	29.12	0.806	29.32	0.809	30.39	0.853

Proposed(*)

SRTV, and its variants, SRTV+BM3D and SRTV+BM3D^2 are validated by comparing the objective and subjective performance with TV [6], as listed in Table 1.

4.1 Parameter Setting for the Experiment

For parameter setting for a original (high) solution image of $2n \times 2n$, $(n = 256)$, the Kronecker compressive sensing measurements was obtained by R_{HR} and G_{HR} with a size, $\lceil 2n\sqrt{r} \rceil \times 2n$, where r denotes an intended subrate of the HR image and $\lceil \cdot \rceil$ stands for ceiling operator. The HR compressive measurements were the same as the LR compressive measurements generated from the Gaussian matrices using the proposed approach, R_{LR} and G_{LR}, at subrate $4r$ with a size of $\lceil 2n\sqrt{r} \rceil \times n$. The reconstruction parameters were set up as $\lambda = 0.5$, $\nu = 0.05$, $\mu = 1$ for all the recovery algorithms and residual reconstructions as well. The stopping criteria for TV reconstruction is 4×10^{-5} and for BM3D post-processing was $tol < 0.002$, and $\sigma = 10$. All results were obtained by averaging five simulations.

Table 3 compares the values of PSNR and the structure similarity index (SSIM) [16] with test images of size 512×512 at various subrates from 0.05 to 0.025. Fig. 3 presents all the test images. The proposed algorithm was compared with TVAL3 [18] with a block size of 64 and BCS-SPL-DDWT with a block size of 32 because the frame-based CS could not be used due to out of memory problems. The experimental environment was a computer with an Intel(R) Core(TM) i5 (3.3GHz) and 4G memory, running Windows 7 and Matlab 2012b.

4.2 Results and Discussions

As shown in Table 3, the SRTV, SRTV+BM3D and SRTV+BM3D^2 algorithms outperformed the conventional method, TV [6], BCS-SPL-DDWT [2], and TVAL3 [18]. Moreover, the SRTV+BM3D^2 showed the best performance in most cases. The results show that the proposed idea of sensing the LR with a high subrate shows better performance than the conventional CS. Even by applying a simple SR (*e.g.*, bi-cubic) to the reconstructed LR image in the SRTV algorithm, the 1.5dB gain on average over the conventional KCS employing TV was still achieved [6]. With the structure preserving property of BM3D post-processing to the LR image, the SRTV+BM3D gives an additional gain of 0.3dB. By building the HR sensing matrix as in (7), it is possible to doubly apply BM3D post-processing to both LR and HR images in the proposed SRTV+BM3D^2, which can offer up to 2.7dB gain (in the case of Cameraman image at subrate 0.25) over the single application of the BM3D post-filter in SRTV+BM3D. In particular, the proposed SRTV+BM3D^2 algorithm demonstrated the best PSNR performance in most test images with a mean gain of 2.94dB and 1dB over the TV [6] and SRTV+BM3D, respectively.

Because only a LR image was measured and a simple SR technique (*e.g.*, bi-cubic) was used to generate the HR image, the HR image often suffers from loss of image details or texture (*i.e.*, due to loss of high frequency components). In addition, the SR technique was reported to generate a smooth HR image and is quite effective in up-sampling a smoothed image [8]. Therefore, the proposed method performs the best with very smooth images, such as Peppers, Cameraman, and Goldhill. The conventional KCS is unable to capture and recover high frequency components well (*e.g.*, edges or details) if it senses a very small number of measurements (*i.e.*, at a very low subrate). Therefore, the reconstructed image of the conventional CS at a very low subrate loses the high frequency components and produces a very low quality reconstructed image, as already visualized in Fig. 1.

Therefore, some high frequency information was discarded using the proposed HR sensing matrix, which corresponds to the sense LR at a high subrate. Because the CS reconstruction works well at a high subrate and the SR technique can provide some level of detail, even without post-processing in the SRTV algorithm, it can still improve the performance in complex textured images, such as the Lena and Boats images. Obviously, higher performance can be achieved with SRTV+BM3D and SRTV+BM3D^2 by exploiting the structures of the image via BM3D. The proposed algorithm can reconstruct both LR and HR images with high quality, as shown in Fig. 4 (Cameraman image at subrate 0.1).

Table 4 lists the reconstruction time of the LR and HR images using various reconstruction algorithms. The reconstructed LR images could be obtained within approximately 3 seconds (in SRTV), 14 seconds (in SRTV+BM3D and SRTV+BM3D^2) with and without BM3D processing. In addition, the computational complexity of the reconstructing HR images ranged from 4 secs in SRTV to 16 sec in SRTV+BM3D, and 85 sec in SRTV+BM3D including the LR reconstruction time. Therefore, an appropriate reconstruction method can be chosen based on the computational capability of the decoder. As shown in Table 5, a very high performance LR image can be obtained using the proposed framework.

In addition, the same conclusion can be drawn in terms

Table 4. Reconstruction time (sec) of the LR and HR Lena image at a subrate 0.05 and 0.15.

Algorithm	HR Reconstruction		LR Reconstruction	
	0.05	0.15	0.05	0.15
BCS-SPL[2]	51.65	24.98	-	-
TVAL3[18]	18.36	37.43	-	-
TV[6]	38.40	26.02	-	-
SRTV*	3.27	3.08	3.26	3.07
SRTV+BM3D*	15.02	14.83	14.99	14.82
SRTV+BM3D^2*	85.12	85.70	15.08	14.96

Proposed(*)

Table 5. Performance of the LR image with/without post processing BM3D in PSNR (dB).

Algorithm		Subrate				
		0.05	0.10	0.15	0.20	0.25
Lena	w/o BM3D	28.32	33.01	37.32	42.57	64.78
	with BM3D	30.08	34.65	38.63	43.24	52.38
Barbara	w/o BM3D	24.81	27.94	31.35	36.81	57.56
	with BM3D	26.03	30.33	35.07	40.47	51.39
Peppers	w/o BM3D	29.00	34.36	38.66	43.54	65.86
	with BM3D	31.32	36.16	39.72	43.82	52.46
Cameraman	w/o BM3D	28.11	33.59	37.96	42.81	63.99
	with BM3D	29.73	34.73	38.52	42.92	52.67
Goldhill	w/o BM3D	26.73	30.49	34.15	38.92	64.43
	with BM3D	27.46	31.13	34.46	39.09	50.29
Boats	w/o BM3D	25.58	29.90	34.25	39.91	62.57
	with BM3D	26.24	30.61	34.89	40.06	50.81

woBM3D (SRTV), wBM3D (SRTV+BM3D and SRTV+BM3D^2)

Fig. 3. From Left to right and up to down are Lena, Barbara, Peppers, Cameramen, Goldhill and Boats test images of size 512x512.

Low resolution image (256x256) High resolution image (512x512)

Fig. 4. Reconstructed image by SRTV+BM3D^2 at subrate 0.1

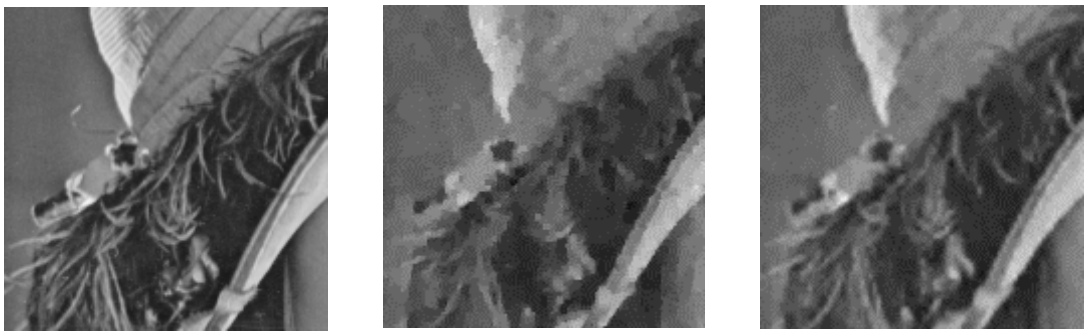

Original TV[6], 28.06dB SRTV, 30.15dB

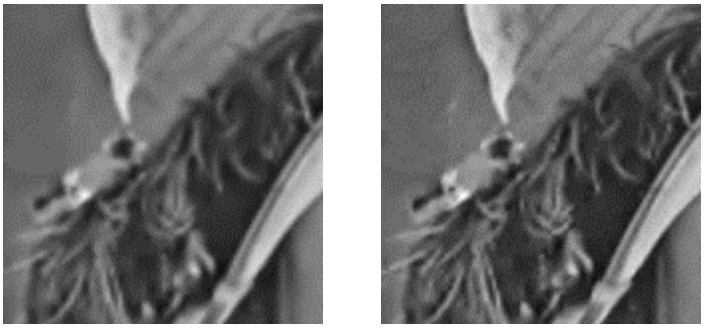

SRTV+BM3D, 30.88dB SRTV+BM3D^2, 32.31dB

Fig. 5. Visual quality comparison of several reconstruction algorithms at subrate 0.1

of the visual quality performance of the reconstruction algorithms, as depicted in Fig. 5 for the Lena image. Obviously, the proposed algorithm produced the best visual quality with clearer textured regions (*e.g.*, see Lena's hair and her hat) and fewer staircase artifacts. However, the reconstructed HR loses some high frequency information (*e.g.*, see the details of Lena's hat, and blurring in Lena's hair region). Moreover, the simple SR technique, such as like bi-cubic interpolation would also smooth the edges in the HR image. Therefore, some high frequency information, such as edges and detail, are lost in the reconstructed HR image. In general, higher recovery performance of the HR image is expected by the better performing SR method. Nevertheless, the task of better preserving the details will be undertaken in future work.

5. Conclusion

This paper proposed a novel multi-resolution Kronecker compressive sensing that allowed simple spatially scalable compressive imaging. The proposed scheme not only provided a high quality low resolution image but also significantly improved the reconstruction

performance of the high resolution image, particularly with a small number of measurements. A future study will extend this sampling scheme further to obtain a scalable compressive sensing framework and exploit predictive coding between the base layers and enhancement layers.

Acknowledgement

This research was supported by the National Research Foundation of Korea (NRF) grant funded by the Korean government (MSIP) (No. 2011-001-7578)

References

[1] D. Donoho, "Compressed sensing," *IEEE Trans. Info. Theory*, vol. 52, no. 4, pp. 1289–1306, 2006. Article (CrossRef Link)

[2] S. Mun and E. Fowler, "Block compressed sensing of images using directional transforms," in Proc. *IEEE Intern. Conf. on Image Process.(ICIP)*, pp. 3021-3024, USA, 2009. Article (CrossRef Link)

[3] K. Q. Dinh, H. J. Shim, and B. Jeon, "Measurement coding for compressive Imaging based on structured measuremnet matrix," in Proc. *IEEE Intern. Conf. on Image Process.(ICIP)*, pp. 10-13, 2013. Article (CrossRef Link)

[4] M. Duarte and R. Baraniuk, "Kronecker compressive sensing," *IEEE Trans. Image Process.*, vol.21, no.2, pp. 494–504, 2012. Article (CrossRef Link)

[5] T. Goldstein and S. Osher, "The split Bregman method for L1 regularized problems," *SIAM J. on Imaging Sci.*, vol. 2, no. 2, pp. 323-343, 2009. Article (CrossRef Link)

[6] S. Shishkin, H.Wang, and G. Hagen, "Total variation minimization with separable sensing operator," in Proc. *Conf. on Image and Signal Process.(ICISP)*, pp. 86–93, 2010. Article (CrossRef Link)

[7] T. N. Canh, K. Q. Dinh and B. Jeon, "Total variation for Kronecker compressive sensing with new regularization," in Proc. *Pic. Coding Symp.(PCS)*, pp. 261-264. 2013. Article (CrossRef Link)

[8] A. K. Katsagellos, R. Mollina, and J. Mateos, Super-Resolution of Images and Video, Morgan & Claypool, 2007. Article (CrossRef Link)

[9] K. Dabov, A. Foi, V. Katkovnik, and K. Egiazarian, "Image denoising by sparse 3D transform-domain collaborative filtering," *IEEE Trans. Image Process.*, vol. 16, no. 8, pp. 2080-2095, 2007. Article (CrossRef Link)

[10] Y. Kim, H. Oh, and A. Bilgin, "Video compressed sensing using iterative self-similarity modeling and residual reconstruction," *J. of Electron. Imaging*, vol. 22. no.2, pp. 021005, 2013. Article (CrossRef Link)

[11] D. Valseia and E. Magli, "Spatially scalable compressed image sensing with hybrid transform and inter-layer prediction model," in *IEEE Inter. Workshop on Multimedia Signal Process.(MMSP)*, pp. 373-378, 2013. Article (CrossRef Link)

[12] A. Sankaranarayanan, C. Studer, and R. Baraniuk, "CS-MUVI: Video compressive sensing for spatial-multiplexing cameras," in *IEEE Inter. Conf. Computational Photography (ICCP)*, pp. 1-10, Apr. 2012. Article (CrossRef Link)

[13] T. Goldstein, L. Xu, K. F. Kelly, and R. G. Baraniuk, "The STONE transform: multi-resolution image enhancement and real-time compressive video," *Available at Arxiv.org (arXiv:1311.3405)*, 2013. Article (CrossRef Link)

[14] M. F. Duarte, M. A. Davenport, D. Takhar, J. N. Laska, T. Sun, K. F. Kelly, and R. G. Baraniuk, "Single-pixel imaging via compressive sampling," *IEEE Signal Process. Mag.*, vol. 25, pp. 83–91, 2008. Article (CrossRef Link)

[15] Z. Wang, A. Bovik, H. Sheikh, and E. Simoncelli, "Image quality assessment: From error measurement to structural similarity," *IEEE Trans. Image Process.*, vol. 13, no. 4, pp. 600-612, 2004. Article (CrossRef Link)

[16] R. G. Keys, "Cubic Convolution Interpolation for Digital Image Proceeding," *IEEE Transactions on Acoustics, Speech, Signal Process.*, vol. 29, no. 6, pp. 1153-1160, 1981. Article (CrossRef Link)

[17] J. Y. Park and M. B. Wakin, "A multiscale framework for compressive sensing of video," in Proc. of *Pict. Coding Symp.(PCS)*, pp. 1-4, 2009. Article (CrossRef Link)

[18] C. Li, W. Yin and Y. Zhang, "An efficient augmented Lagragian method with applications to total variation minimization," in *Comput. Optimization and Application*, vol. 56, not. 3, pp. 507-530, 2013. Article (CrossRef Link)

Thuong Nguyen Canh received his B.S. in Electronics and Telecommunications from Hanoi University of Science and Technology, Hanoi, Vietnam in 2012. He is currently a master's student in Electrical and Computer Engineering at Sungkyunkwan University, Suwon, Korea. His current research involves image/video compression and compressed sensing.

Khanh Quoc Dinh received his B.S. degree in Electronics and Telecommunications from the Hanoi University of Science and Technology, Hanoi, Vietnam, in 2010, the B.S. degree in Electrical and Computer Engineering from Sungkyunkwan University, Suwon, Korea, in 2012. He is currently a Ph.D. candidate in the Digital Media Laboratory at Sungkyunkwan University. His research interests include video compression and compressive sensing.

Byeungwoo Jeon received his BS degree in 1985 and an MS degree in 1987 from the Department of Electronics Engineering, Seoul National University, Seoul, Korea. He received his PhD degree in 1992 from the School of Electrical Engineering at Purdue University, Indiana, United States. From 1993 to 1997 he was in the Signal Processing Laboratory at Samsung Electronics in Korea, where he worked on video compression algorithms, designing digital broadcasting satellite receivers, and other MPEG-related research for multimedia applications. Since September 1997, he has been with the faculty of the School of Electronic and Electrical Engineering, Sungkyunkwan University, Korea, where he is currently a professor. His research interests include multimedia signal processing, video compression, statistical pattern recognition, and remote sensing.